

Simulation of Sensor Application and Shape Control of Piezoelectric Structures at Large Deflections.

S. Lentzen¹, R. Schmidt¹

Summary

A geometrically non-linear finite element method is proposed to investigate composite shell structures with integrated piezoelectric layers. The strain displacement relations are based on a moderate rotation theory and the Reissner Mindlin hypothesis. The internal and external virtual work is calculated using the total Lagrangian formulation. Two examples are presented to demonstrate the effect of the geometrical non-linearity on actuator and sensor applications of the piezoelectric layers.

Introduction

The aim of modern designing is to reduce the weight of structures as well as the raw material needed for manufacturing. This leads to light-weight structures which are sensitive to stability problems as well as oscillations. In recent years much research has been conducted in the area of smart materials and structures to overcome this weakness. The theory of piezoelectric plates and shells in the geometrically linear range of deformation is extensively treated by Tzou [6] amongst others. Considerably less work can be found in the area of geometrically non-linear theories, e.g. [1], [2] and [5]. In this work an approach to FE simulation of sensor application and shape control is demonstrated based on non-linear shell theory. In a similar way recently Mukherjee et al. [2] have demonstrated the geometrically non-linear sensor application based on von Kármán type non-linear beam theory, and Lee et al. [3] have treated shape control based on linear degenerated shell elements.

Electromechanical equations

The virtual work principle states a state of equilibrium between the external virtual work δW_e and internal virtual work δW_i . In the present work a total Lagrangian formulation is chosen. For this approach the mechanical and electrical quantities need to be defined with reference to the undeformed configuration, denoted by the lower left subscript 0, and integration is performed over the undeformed volume and surfaces. The internal virtual work is the volume integral of the virtual electric enthalpy δH and it can be written as:

$$\delta W_i = \int_V \delta H dV \quad \text{with} \quad \delta H = {}_0\sigma^{ij} \delta \varepsilon_{ij} - {}_0D^i \delta E_i, \quad (1)$$

where ${}_0\tilde{\sigma}$ denotes the 2nd Piola-Kirchhoff stress tensor, ${}_0\tilde{\varepsilon}$ is the Green-Lagrange strain tensor, ${}_0\tilde{D}$ denotes the electric displacement vector and ${}_0\tilde{E}$ is the electric field vector. The

¹Institute of General Mechanics, RWTH Aachen University, Aachen, Germany

latter is calculated as the gradient of the electric potential ϕ in the undeformed configuration

$${}^0\tilde{E} = -\text{GRAD}(\phi). \quad (2)$$

The Green-Lagrange strain tensor components with the assumption of first-order shear deformation theory, small strains but moderate rotations are expressed as [4]:

$$\begin{aligned} \varepsilon_{\alpha\beta} &= {}^0\varepsilon_{\alpha\beta} + \Theta^3 {}^1\varepsilon_{\alpha\beta} + (\Theta^3)^2 {}^1\varepsilon_{\alpha\beta} \\ \varepsilon_{\alpha 3} &= {}^0\varepsilon_{\alpha 3} + \Theta^3 {}^1\varepsilon_{\alpha 3} \\ \varepsilon_{33} &= 0 \end{aligned} \quad (3)$$

with

$$\begin{aligned} {}^0\varepsilon_{\alpha\beta} &= \theta_{\alpha\beta} + \frac{1}{2} \Phi_{\alpha}^0 \Phi_{\beta}^0, \\ {}^1\varepsilon_{\alpha\beta} &= \frac{1}{2} \left(v_{\alpha|\beta}^1 + v_{\beta|\alpha}^1 - b_{\alpha}^{\lambda} \Phi_{\lambda\beta}^0 - b_{\beta}^{\lambda} \Phi_{\lambda\alpha}^0 + \Phi_{\alpha}^0 b_{\beta}^{\lambda} v_{\lambda}^1 + \Phi_{\beta}^0 b_{\alpha}^{\lambda} v_{\lambda}^1 \right), \\ {}^2\varepsilon_{\alpha\beta} &= \frac{1}{2} \left(b_{\alpha}^{\lambda} b_{\beta}^{\kappa} v_{\lambda}^1 v_{\kappa}^1 - b_{\alpha}^{\lambda} v_{\lambda|\beta}^1 - b_{\beta}^{\lambda} v_{\lambda|\alpha}^1 \right), \\ {}^0\varepsilon_{\alpha 3} &= \frac{1}{2} \left(\Phi_{\alpha}^0 + v_{\alpha}^1 + v^{\lambda} \Phi_{\lambda\alpha}^0 \right) \quad \text{and} \quad {}^1\varepsilon_{\alpha 3} = \frac{1}{2} v^{\lambda} v_{\lambda|\alpha}^1. \end{aligned}$$

The following abbreviations are used:

$$\begin{aligned} \theta_{\alpha\beta} &= \frac{1}{2} \left(v_{\alpha|\beta}^0 + v_{\beta|\alpha}^0 \right) - b_{\alpha\beta}^0 v_3, \\ \Phi_{\alpha\beta}^0 &= v_{\alpha|\beta}^0 - b_{\alpha\beta}^0 v_3 \quad \text{and} \quad \Phi_{\alpha}^0 = v_{3,\alpha}^0 + b_{\alpha}^{\lambda} v_{\lambda}^0, \end{aligned}$$

where $b_{\alpha\beta}$ and b_{β}^{α} denote the covariant and mixed components of the curvature tensor and $(\cdot)_{|\alpha}$ is the covariant derivative with respect to the surface parameter Θ^{α} . The translation of the midsurface in direction of Θ^i is denoted with v_i^0 and the rotation of the normal in direction Θ^{α} with v_{α}^1 .

Constitutive Relations

The piezoelectric effect is described by the following set of linear constitutive equations in vector form:

$$\{ {}_0D \} = [e] \{ {}_0\varepsilon \} + [\delta] \{ {}_0E \} \quad (4)$$

$$\{ {}_0S \} = [c] \{ {}_0\varepsilon \} - [e]^T \{ {}_0E \} \quad (5)$$

where $\{ {}_0S \}$ denotes the stress vector, $\{ {}_0\varepsilon \}$ the strain vector, $\{ {}_0D \}$ the electric displacement vector and $\{ {}_0E \}$ the electric field vector.

$$\{ {}_0S \} = \begin{Bmatrix} \sigma^{11} \\ \sigma^{22} \\ \tau^{12} \\ \tau^{23} \\ \tau^{13} \end{Bmatrix}, \{ {}_0\varepsilon \} = \begin{Bmatrix} \varepsilon_{11} \\ \varepsilon_{22} \\ 2\varepsilon_{12} \\ 2\varepsilon_{23} \\ 2\varepsilon_{13} \end{Bmatrix}, \{ {}_0D \} = \begin{Bmatrix} D^1 \\ D^2 \\ D^3 \end{Bmatrix}, \{ {}_0E \} = \begin{Bmatrix} E_1 \\ E_2 \\ E_3 \end{Bmatrix}$$

Further $[e] = [d][c]$ and $[e]^T = [c][d]^T$, $[c]$ denotes the elasticity matrix for anisotropic material, $[d]$ the piezoelectric constant matrix and $[\delta]$ the dielectric constant matrix

$$[c] = \begin{bmatrix} c_{11} & c_{12} & c_{13} & 0 & 0 \\ c_{12} & c_{22} & c_{23} & 0 & 0 \\ c_{13} & c_{23} & c_{33} & 0 & 0 \\ 0 & 0 & 0 & c_{44} & c_{45} \\ 0 & 0 & 0 & c_{45} & c_{55} \end{bmatrix}, [d]^T = \begin{bmatrix} 0 & 0 & d_{31} \\ 0 & 0 & d_{31} \\ 0 & 0 & 0 \\ 0 & d_{15} & 0 \\ d_{15} & 0 & 0 \end{bmatrix},$$

$$[\delta] = \begin{bmatrix} \delta_{11} & 0 & 0 \\ 0 & \delta_{22} & 0 \\ 0 & 0 & \delta_{33} \end{bmatrix}.$$

It is assumed that the electric field is only existent in transverse direction and homogeneous between the poles of an electrode pair. In the present work the electromechanical system is treated in a decoupled way. The actuators are voltage driven and the influence of the generated electric field of the sensors on the mechanical stresses is assumed to be negligible.

Examples

Two examples, the geometry and material properties of which are given in Figure (1) and Table 1, are considered. Figure 2 refers to the cantilever beam and displays the results of two cases. On the left hand side the sensor voltages are displayed in case the beam is loaded with a tip force of 2.5 N and the upper PZT layer is subdivided into 10 equal

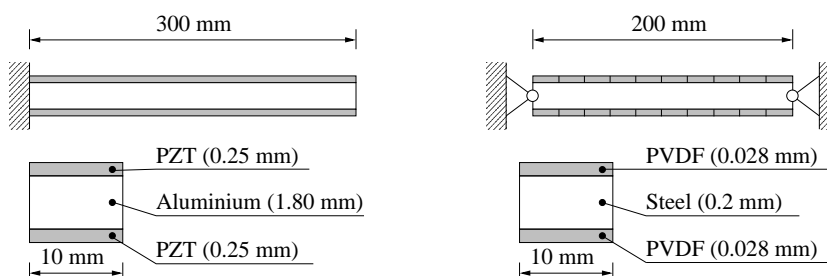


Figure 1: Two examples: a cantilever beam and a hinged beam.

Table 1: Material properties.

	E [GPa]	ν [-]	d_{31} [Cb/N]	δ_{33} [F/m]
aluminium	65	0.3	-	-
steel	210	0.3	-	-
PZT	63	0.3	$1.66 \cdot 10^{-11}$	$1.59 \cdot 10^{-8}$
PVDF	2	0.3	$2.2 \cdot 10^{-11}$	$1.06 \cdot 10^{-10}$

electrode pairs. At this load a clear difference is noticed between the geometrically linear approach and the moderate rotation theory. Due to stress stiffening the deformations in the non-linear case are smaller, which explains smaller sensor voltages than predicted by linear theory. The graph on the right hand side shows the deformed configuration when the beam is loaded by a tip force of 0.01 N and the lower PZT layer is actuated such that the tip deflection remains zero. Two cases are considered in which the actuator layer consists of either one patch over the length of the beam or 10 equal patches. In the first case an actuation voltage of 92.68 V has to be applied to reduce the tip deflection to zero. In the latter case the actuation voltages are applied proportionally to the sensor voltages in the left graph. The maximum voltage of 269.07 V has to be applied in order to reduce the tip deflection to zero. The results are only shown for the linear case, since the deflections are small. Deflections in the range of non-linear theory would require too high actuating voltages. Figure 3 refers to the hinged beam. In the upper left corner the results are displayed when both PVDF layers are actuated. The non-dimensionalised mid-point deflection and longitudinal stress at the mid-surface are shown. In the linear case, i.e. for the pure bending problem, the stress is expected to be zero. One can observe that a longitudinal stress develops when the non-linear solution diverges from the linear one. This reflects the von Kármán effect and indicates that additional tensile forces are induced in the geometrically non-linear range of deformation. A very good agreement is obtained with [1] where finite elements based on non-linear beam theory have been used. In the upper right corner the sensor voltages in the upper PVDF layer, subdivided into 10 equal electrode pairs, are displayed when a force of 0.001 N is applied in the mid-point. Again, due to stress stiff-

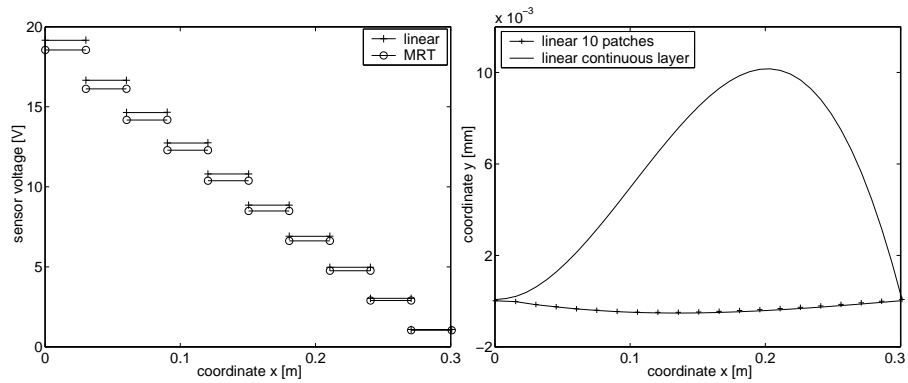


Figure 2: left: sensor voltages at 2.5 N, right: piezoelectrically activated beam at 0.01 N.

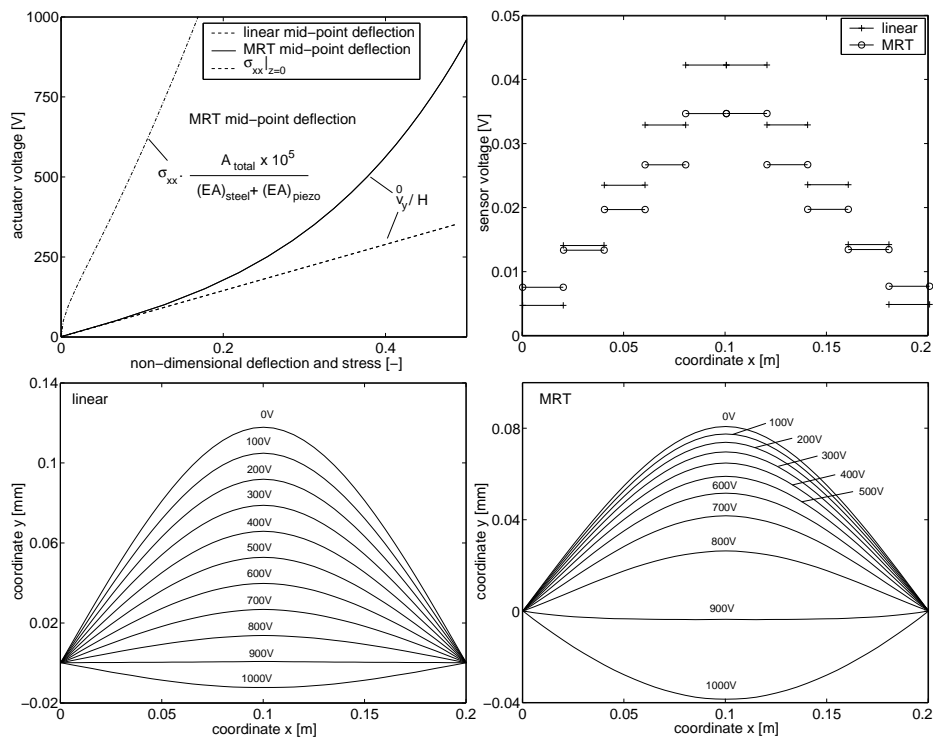


Figure 3: upper left: non-dimensional mid-point deflection and longitudinal stress, upper right: sensor voltages at 0.001 N in the mid-point, lower left and right: piezo-electrically activated beam at 0.001 N (linear and MRT analysis).

ening the deformations predicted by non-linear analysis, and hence the sensor voltages, are smaller than those predicted by linear theory in most areas of the beam, except of the boundary, where tensile forces dominate which are not accounted for by linear analysis. Next, once again it is assumed that the lower PVDF layer consists of 10 equal patches and a voltage proportional to the respective sensor output is applied until the beam is flattened. The results are displayed in the two lower graphs. The deformed beam is shown with the associated maximum applied voltages. In contrast to the cantilever beam, here the deflections are in the range of geometrically non-linear theory. Therefore the results of linear and MRT analysis differ significantly. Linear analysis overpredicts by far the deformations.

Conclusions

A geometrically non-linear finite element method is proposed to investigate composite shell structures with integrated piezoelectric layers. By means of two examples a clear difference between a geometrically linear and a non-linear approach in the simulation of structures with integrated piezoelectric layers is demonstrated.

Reference

1. Chróscielewski, J., Klosowski, P. and Schmidt, R. (1997): "Modelling and FE-Analysis of Large Deflection Shape and Vibration Control of Structures via Piezoelectric Layers.", *Fortschritts-Berichte VDI*, Vol. 11, pp. 53–62.
2. Mukherjee, A. and Chaudhuri, A.S. (2002): "Piezolaminated Beams with Large Deformations.", *Int.J. of Solids and Structures*, Vol. 39, pp. 1567-4582.
3. Lee, S., Goo, N.S., Park, H.C., Yoon, K.J. and Cho, C. (2003): "A Nine-Node Assumed Strain Shell Element for Analysis of a Coupled Electro-Mechanical System.", *Smart. Mater. Struct.*, Vol. 12, pp. 355-362.
4. Schmidt, R. and Reddy, J. N. (1988): "A Refined Small Strain and Moderate Rotation Theory of Elastic Anisotropic Shells", *Journal of Applied Mechanics*, Vol. 55, pp. 611-617.
5. Shi, G. and Atluri, S.N. (1990): "Active Control of Nonlinear Dynamic Response of Space-Frames Using Piezo-Electric Actuators" *Computers & Structures*, Vol. 34, pp. 549-564.
6. Tzou, H.S. (1993): *Piezoelectric Shells*, Kluwer Academic Publishers.